CAPABILITY OF MODERN IN SITU DIAGNOSTICS FOR THE ANALYSIS OF THE SC ANTISOLVENT (SAS) TECHNOLOGY

A. Braeuer*, S. Dowy, and A. Leipertz
Lehrstuhl für Technische Thermodynamik and Erlangen Graduate School in Advanced Optical Technologies (SAOT), Universität Erlangen-Nürnberg, Am Weichselgarten 8, 91058 Erlangen, Germany
ab@ltt.uni-erlangen.de & 0049 9131 8525853

Optical diagnostics are useful tools, to in-situ study the mechanisms taking place inside the supercritical antisolvent (SAS)-vessel during particle precipitation. We report the capability of modern in-situ diagnostics for the analysis of the SAS-technology. A linear Raman imaging technique is introduced to simultaneously image the mixture composition (mole fraction), the partial density of CO_2, the position of first precipitation and the solute's concentration within the SAS-vessel.

An elastic light scattering technique is introduced to analyze, whether the transient interfacial tension between the injected solution and the $scCO_2$ decays to zero before or after jet break up, and therefore is the switch criterion between the formation of droplets or no formation of droplets.

An absorption/emission technique, which is based on the Foerster Resonant Energy Transfer (FRET) between a donor and an acceptor chromophor, is introduced to analyze the absorption of CO_2 in the injected liquid solution and the subsequent evaporation of solvent from the liquid droplet.

INTRODUCTION

In the supercritical antisolvent (SAS)-process particles are usually processed under high pressure conditions in compact vessels. Therefore the mechanisms taking place inside the vessel remain sealed and thus the attempts to understand the SAS process are very often based on thermodynamic knowledge which is only true for equilibrium conditions. To study the transient and turbulent mechanisms inside the SAS vessel when the solution is injected into sc carbon dioxide ($scCO_2$), some research groups equipped their SAS vessels with windows to provide optical access [1-7]. Nevertheless, the vast majority of reported optical observations are rather qualitative and lack quantitative information about the injection, the mixing and the precipitation mechanisms.

Since 2005 we are developing and carrying out in situ optical diagnostics to study the SAS-precipitation regarding the injection event, the mixing mechanisms and the precipitation event. In contrast to investigations of other research groups our measurement techniques provide quantitative information with a high temporal and spatial resolution [8-15]. From our investigations quantitative information on flow field, jet break up, density, composition, mass transfer, interfacial tension and volume expansion can be extracted. The different measurement techniques are based on advanced light scattering and absorption/emission techniques.

This contribution aims to provide a general survey on the capability of modern in situ optical diagnostics for the analysis of the SAS-technology.

ELASTIC LIGHT SCATTERING FOR JET BREAK UP ANALYSIS

In collaboration between the research group of Professor Reverchon from the University Salerno (Fisciano/Italy) and our research group, an experimental setup as given in Figure 1, was used to analyze the jet break up phenomena and to correlate them with the resulting particles' morphologies.
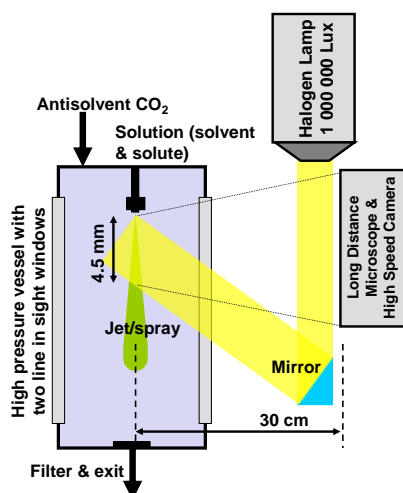

Figure 1 Schematic of the experimental setup

An optical accessible high pressure chamber, with two windows orientated line in sight was used as SAS precipitator. The solution, which is composed of an organic solvent and a solute, is injected in the supercritical antisolvent CO_2. The injected jet was observed between the nozzle outlet and 4.5 mm downstream by applying an elastic light scattering setup. The jet was illuminated under a certain angle from the bottom. Elastically scattered light (Rayleigh-, Mie-, and optical scattering) is imaged via a long distance microscope onto the CMOS-chip of a high speed camera and detected. Details on the respective light matter interactions are given in [16].

Figure 2 summarizes the different mixing behaviours of the injected solvent jet, which is observed when using Mie- and Rayleigh scattering images; e.g,. jet break-up into rather large droplets (drops) at a certain distance from the nozzle (Figure 2a), jet atomization into small droplets, which cannot be resolved by the microscope (Figure 2b), and "gas-plume" like mixing, when no droplets are formed (Figure 2c).
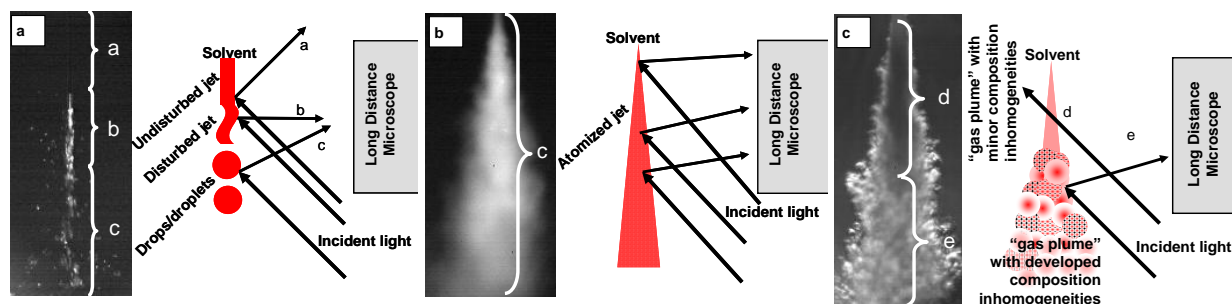

Figure 2 Elastic light scattering images and sketches of the light scattering mechanism for operation conditions, where the jet disintegrates in drops (Figure 2a), where the jet is atomized into droplets (Figure 2b) and where the jet mixes in a single phase (Figure 2c).

Figure 3 shows the jet behaviour at different pressures operating at 40°C and for a DMSO flow rate of 2.5 mL min^{-1} through the 80 µm nozzle.
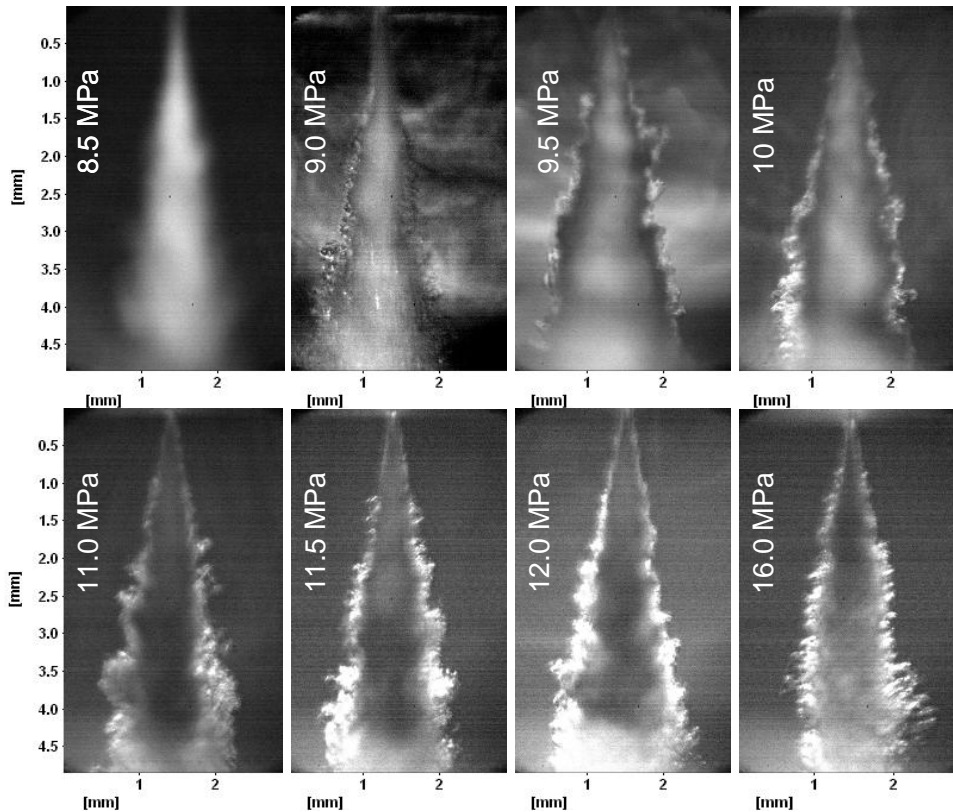
Figure 3 Elastic light scattering images, when DMSO is injected with a flow rate of 2.5 mL min^{-1} into pressurized CO_2 through a 80 µm nozzle at 313 K. The pressure of CO_2 was varied as given in the corresponding images.

At 8.5 MPa (at subcritical conditions) a dense droplet laden spray can be identified. Single droplets are not detectable, but intense Mie scattering signals proof their existence. Therefore, jet mixing at 8.5 MPa clearly takes place in a multi-phase flow. At 9.0 MPa, the jet already has characteristics of both, multi-phase mixing in the jet centre with Mie scattering signals and single-phase mixing at the jet edges with Rayleigh scattering signals. Within the jet core, bright Mie scattering signals proof the presence of small droplets. There is a narrow dark gap between the Mie scattering signals in the jet core and the Rayleigh scattering signals at the jet edges. Increasing the pressure, the dark gap, which indicates the transition from multi-phase to single-phase mixing, enlarges between the jet centre and the jet edges. Up to 12 MPa there is still a Mie scattering signal detectable at the jet centre, in the upper part of the jet images (weak but detectable), due to the presence of droplets. At pressures exceeding 12 MPa, for example at 16 MPa, the jet consists only of "parts d" and "part e" as described in Figure 2. Consequently at 16 MPa, jet mixing takes place completely within a homogeneous single-phase. This series of images demonstrates that in the case of DMSO at pressures larger than the MCP a progressive transition exists between multi-phase and single-phase mixing. It ends at pressures of approximately 12 MPa.

Therefore, when operating below a pressure of 12 MPa, the precipitation kinetics of the solute govern, whether the precipitation takes place in droplets (close to the injection nozzle where droplets are still detectable), or in a gas-plume like environment, when the transient interfacial tension between the bulk CO_2 and the injected solution is already diminished. As a consequence, spherical mico-particles result from fast precipitation kinetics in droplets and amorphous nano-particles result from slow precipitation kinetics in the gas-plume-like environment. Summarizing, we were able to explain the occurrence of different particle

3

morphologies for operation conditions above the mixture critical point of the binary solvent/antisolvent mixture. A more comprehensive study of the disappearance of the transient interfacial tension and their impact for jet mixing is given in [16].

FRET TO IN-SITU ANALYZE MASS TRANSPORT ACROSS PHASE BOUNDARIES

If the solution is injected into the sc antisolvent below the mixture critical pressure, droplets are formed after jet break-up [13, 14]. Foerster resonant energy transfer (FRET) which is a dipole/dipole interaction between a donor and an acceptor molecule is a widespread technique in molecular biology to analyze intermolecular mechanisms [17]. The FRET efficiency is highly sensitive to the distance between the donor and the acceptor molecules [18] and can be determined from the donor/acceptor fluorescence emission spectra.

In the case of supercritical particle technology the solute can be replaced by donor and acceptor dye molecules. Volume expansion and reduction which occurs during the mixing of the donor/acceptor (d/a)-solution with the $scCO_2$ manipulates the intermolecular distance between the two dye molecules. Consequently, the volume alteration of the liquid phase can be extracted from the fluorescence emission spectrum of the d/a-solution.

Rhodamine B (RhB) and Rhodamine 700 (Rh700) were chosen here as donor/acceptor-couple because of several reasons. Firstly, the donor molecule RhB can easily be excited to fluorescence with common green laser sources, e.g. a frequency-doubled Nd:YAG-laser at 532 nm. Secondly, the RhB emission spectrum and the Rh700 absorption spectrum show a wide overlap which proofs their suitability as a FRET d/a-couple. Thirdly, RhB and Rh700 feature high solubility in most organic solvents. And fourthly, both dye molecules are non-soluble in $scCO_2$. Consequently, all RhB and Rh700 molecules remain inside the liquid phase during volume expansion and do not travel across the phase boundary into the $scCO_2$.

Details regarding the experimental setup, the calibration and the data evaluation will be provided in a future publication.

Nevertheless, the capability of FRET diagnostics is expressed in Figure 4, where one can see how the Fluorescence ratio acceptor/donor decreases with increasing chamber pressure.
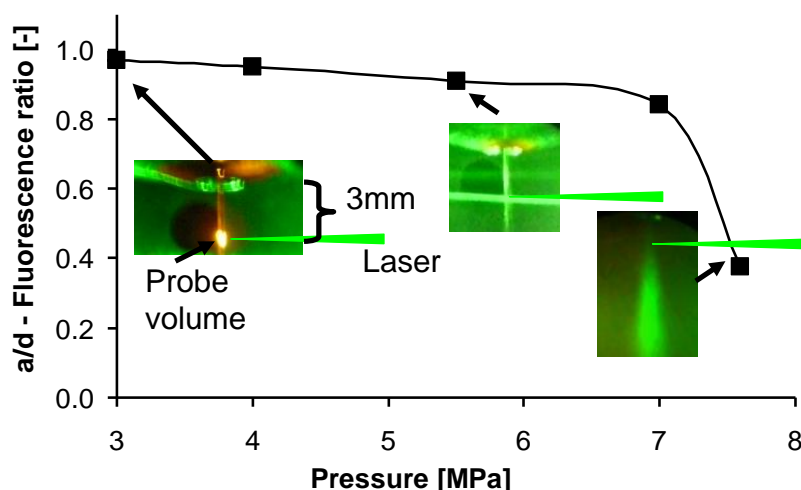

Figure 4 Fluorescence ratio a/d as a function of CO_2 pressure. The fluorescence ratio decrease shows, at which pressure the CO_2 absorption causes volume expansion.

This trend correlates with the volume expansion data of CO_2 pressurized organic solvents [19-21].

RAMAN SCATTERING FOR MULTI-PARAMETER IMAGING

In contrast to Rayleigh-, Mie-, and optical scattering, Raman scattering is an inelastic light scattering mechanism, which means that the signal frequency is frequency shifted from the frequency of the incident radiation. This frequency shift is species specific and therefore different for the solvent and for the antisolvent. Furthermore the Raman scattering intensity linearly scales with the number density of probed molecules, which means, that the corresponding signal intensities are directly proportional to the partial density of either solvent or antisolvent. This is why Raman scattering is a quantifiable optical measurement technique. If it is combined with an optical measurement technique, which qualifies for the detection of phase boundaries (like Mie scattering), two-dimensional information on mole fraction, partial density, supersaturation and the location of first precipitation is accessible. While a combined Raman-Mie experimental setup is rather complex, the evaluation and interpretation of the measurement data is simple. Detailed explanations on this measurement concept are available in [12-15, 22].

REFERENCES:

[1]   E. Badens, O. Boutin, G. Charbit, Laminar jet dispersion and jet atomization in pressurized carbon dioxide, J. Supercrit. Fluids 36 (2005) 81-90.

[2]   S.S. Dukhin, Y. Shen, R. Dave, R. Pfeffer. Droplet mass transfer, intradroplet nucleation and submicron particle production in two-phase flow of solvent-supercritical antisolvent emulsion. 2005: Elsevier Science Bv.

[3]   A. Gokhale, B. Khusid, R.N. Dave, R. Pfeffer, Effect of solvent strength and operating pressure on the formation of submicrometer polymer particles in supercritical microjets, J. Supercrit. Fluids 43 (2007) 341-356.

[4]   L.Y. Lee, L.K. Lim, J. Hua, C.-H. Wang, Jet breakup and droplet formation in near-critical regime of carbon dioxide-dichloromethane system, Chem. Eng. Sci. 63 (2008) 3366-3378.

[5]   C.S. Lengsfeld, J.P. Delplanque, V.H. Barocas, T.W. Randolph, Mechanism governing microparticle morphology during precipitation by a compressed antisolvent: atomization vs. nucleation and growth, J. Phys. Chem. B 104 (2000) 2725-2735.

[6]   D.L. Obrzut, P.W. Bell, C.B. Roberts, S.R. Duke, Effect of process conditions on the spray characteristics of a PLA plus methylene chloride solution in the supercritical antisolvent precipitation process, J. Supercrit. Fluids 42 (2007) 299-309.

[7]   M. Sarkari, I. Darrat, B.L. Knutson, Generation of microparticles using CO2 and CO2-philic antisolvents, Aiche J. 46 (2000) 1850-1859.

[8]   A. Braeuer, S. Dowy, A. Leipertz, R. Schatz, M. Rossmann, D.-Ing E. Schluecker, Optische in-situ-Untersuchungen der Partikelbildung im überkritischen Antisolvent-Prozess, Chemie Ingenieur Technik 81 (2009) 1453-1457.

[9]   A. Braeuer, S. Dowy, A. Leipertz, R. Schatz, E. Schluecker, Injection of ethanol into supercritical CO_2: Determination of mole fraction and phase state using linear Raman scattering, Opt. Express 15 (2007) 8377-8382.

[10]   A. Braeuer, S. Dowy, R. Schatz, M. Rossmann, E. Schluecker, A. Leipertz, Supercritical Antisolvent Particle Precipitation: In Situ Optical Investigations, Chemical Engineering & Technology 9999 (2009) NA.

[11]   A. Braeuer, S. Dowy, R. Schatz, E. Schluecker, A. Leipertz. Antisolvent Precipitation: Interaction of Mixing, Phase behaviour and Particle formation. in 9th international Symposium on Supercritical Fluids. 2009. Arachon: ISASF.

[12]   S. Dowy, A. Braeuer, A. Leipertz. CO_2 partial density distribution under dynamic mixture generation conditions in the supercritical antisolvent process. in 11th European Meeting on Supercritical Fluids. 2008. Barcelona: ISASF.

[13]   S. Dowy, A. Braeuer, K. Reinhold-Lopez, A. Leipertz, Laser analyses of mixture formation and the influence of solute on particle precipitation in the SAS process, J. Supercrit. Fluids 50 (2009) 265-275.

[14]   S. Dowy, A. Braeuer, R. Schatz, E. Schluecker, A. Leipertz, CO_2 partial density distribution during high-pressure mixing with ethanol in the supercritical antisolvent process, J. Supercrit. Fluids 48 (2009) 195-202.

[15]   S. Dowy, A. Braeuer, R. Schatz, E. Schluecker, A. Leipertz. Particle Nucleation and Mixture Formation Characterized by a combination of Raman and Mie Scattering. in 9th international Symposium on Supercritical Fluids. 2009. Arachon: ISASF.

[16]   E. Reverchon, E. Torino, S. Dowy, A. Braeuer, A. Leipertz, Interactions of phase equilibria, jet fluid dynamics and mass transfer during supercritical antisolvent micronization, Chemical Engineering Journal 156 (2010) 446-458.

[17]   C. Kaminski, Quantitative fluorescence microscopy, Journal of The Royal Society Interface 6 (2009) S1-S2.

[18]   T. Förster, Transfer Mechanisms of Electronic Excitation Energy, Radiation Research Supplement 2 (1960) 326-339.

[19]   C.-Y. Day, C.J. Chang, C.-Y. Chen, Phase Equilibrium of Ethanol + CO_2 and Acetone + CO_2 at Elevated Pressures, J. Chem. Eng. Data 41 (1996) 839-843.

[20]   T. Fornari, E.J. Hernández, G. Reglero, Solubility of supercritical gases in organic liquids, J. Supercrit. Fluids 51 (2009) 115-122.

[21]   K. Suzuki, H. Sue, M. Itou, R.L. Smith, H. Inomata, K. Arai, S. Saito, Isothermal vapor-liquid equilibrium data for binary systems at high pressures: carbon dioxide-methanol, carbon dioxide-ethanol, carbon dioxide-1-propanol, methane-ethanol, methane-1-propanol, ethane-ethanol, and ethane-1-propanol systems, J. Chem. Eng. Data 35 (1990) 63-66.

[22]   A. Braeuer, S. Dowy, R. Schatz, M. Rossmann, E. Schluecker, A. Leipertz, Supercritical Antisolvent Particle Precipitation: In Situ Optical Investigations, Chemical Engineering & Technology 33 (2010) 35-38.